

Vision-based quadrotor stabilization using a pan and tilt camera

D. Cabecinhas, C. Silvestre and R. Cunha

Abstract—This paper proposes a nonlinear control architecture for the stabilization of a quadrotor vehicle based on image measurements of a set of landmarks obtained from a pan and tilt camera. The vehicle is stabilized vertically using an additional vertical position sensor and lateral-longitudinal stabilization is achieved with a nested saturation control law by feedback of image measurements, body attitude, and angular rate. Additionally, the pan and tilt camera is actively actuated to keep the landmarks visible in the image sensor for most operating conditions. Simulation results are presented to assess the performance of the proposed control architecture.

I. INTRODUCTION

The operation of Unmanned Aerial Vehicles (UAVs) in indoor and urban environments, where GPS signals are unreliable or simply unavailable, calls for alternative solutions based on local sensor measurements such as vision-based control. Over the years the topic of vision-based control has been extensively studied, experimentally tested, and is well documented (see for example [1], [2] and references therein). The literature on vision-based rigid-body stabilization and estimation highlights important questions and indicates possible solutions to i) keeping feature visibility along the system's trajectories for a large region of attraction [3], [4], ii) minimizing the required knowledge about the 3-D model of the observed object [5], iii) guaranteeing convergence in the presence of camera parametric uncertainty and image measurement noise [5], iv) establishing observability conditions for attitude estimation [6]. More recently, a controller for point stabilization based on backstepping and optical flow was presented in [7].

Besides rigid-body stabilization, vision-based control has been used to accomplish other tasks relying on different image features such as straight line and curve representations [8], [9], image centroids or higher order image moments [10]. For example, in [8] the authors propose an image based control design to track parallel linear features for an underactuated vehicle. A follow-the-leader problem for mobile robots equipped with panoramic cameras is addressed in [11]. In [9], the authors consider the problem of steering a mobile robot to track a curve by controlling the shape of the curve in the image plane. In both [9] and [11], the two-dimensional nature of the problem removes depth ambiguity from the image measurements, which indicates that an extension to 3-D space may not be straightforward.

This work was partially supported by Fundação para a Ciência e a Tecnologia (ISR/IST plurianual funding) and by the project PTDC/EAAACR/72853/2006 HELICIM of the FCT and AIRTICI from AdI.

The work of D. Cabecinhas was supported by a PhD Student Grant from the FCT POCTI program, SFRH / BD / 31439 / 2006.

D. Cabecinhas, C. Silvestre and R. Cunha are with the Department of Electrical Engineering and Computer Science, and Institute for Systems and Robotics, Instituto Superior Técnico, 1049-001 Lisboa, Portugal. {dcabecinhas,cjs,rita}@isr.ist.utl.pt

We are particularly interested in devising strategies for motion control of quadrotors, taking into account both the dynamics and the underactuated nature of the vehicle. Several approaches to quadrotor position tracking have concentrated on using nonlinear techniques, such as backstepping [12], [13] and feedforward control [14], [15], to solve the trajectory tracking problem for a single vehicle.

The main contribution of this paper is the introduction of a feedback control architecture for the design of image based controllers for the stabilization of quadrotor vehicles in hover close to a set of landmarks placed in the terrain. The proposed pan and tilt camera controller diverges from the classic literature [2] as it does not require explicit estimation of the vehicle's position and velocity. The quadrotor stabilization controller imposes a two-time scale dynamics, decoupling the vertical from the lateral-longitudinal subsystem. The vertical controller can be viewed as a time-varying PD controller and a nested saturations control scheme is used to stabilize the lateral-longitudinal subsystem, which has a feedforward structure. Both these controllers diverge from the ones in [14] as only measurements available from the image sensor are used, instead of classic full-state feedback.

II. QUADROTOR MODEL

We model the quadrotor vehicle as a rigid body that is actuated in force and torque. Consider a fixed inertial frame $\{I\}$ and a frame $\{B\}$ attached to the vehicle's center of mass. The configuration of the body frame $\{B\}$ with respect to $\{I\}$ can be viewed as an element of the Special Euclidean group, $(R, \mathbf{p}) = ({}^I_B R, {}^I \mathbf{p}_B) \in \text{SE}(3)$. The kinematic and dynamic equations of motion for the rigid body can be written as

$$\dot{R} = RS(\boldsymbol{\omega}_B) \quad (1)$$

$$\dot{\mathbf{p}} = R\mathbf{v} \quad (2)$$

$$\dot{\boldsymbol{\omega}}_B = -\mathbb{J}^{-1}S(\boldsymbol{\omega}_B)\mathbb{J}\boldsymbol{\omega}_B + \mathbb{J}^{-1}\mathbf{n} \quad (3)$$

$$\dot{\mathbf{v}} = -S(\boldsymbol{\omega}_B)\mathbf{v} + \frac{1}{m}\mathbf{f}, \quad (4)$$

where the position \mathbf{p} is expressed in the inertial frame $\{I\}$, R is the rotation matrix from $\{B\}$ to $\{I\}$, and the angular velocity $\boldsymbol{\omega}_B \in \mathbb{R}^3$ and the linear velocity $\mathbf{v} \in \mathbb{R}^3$ are expressed in the body frame $\{B\}$. The scalar m and the matrix $\mathbb{J} \in \mathbb{R}^{3 \times 3}$ represent the quadrotor's mass and moment of inertia, \mathbf{f} and $\mathbf{n} \in \mathbb{R}^3$ denote respectively the external force and torque expressed in the body frame and $S(\mathbf{x})$ is the skew symmetric matrix defined by the vector $\mathbf{x} \in \mathbb{R}^3$ such that $S(\mathbf{x})\mathbf{y} = \mathbf{x} \times \mathbf{y}$, $\mathbf{y} \in \mathbb{R}^3$. Aerodynamic drag forces due to the fuselage are neglected given the low speeds at which the quadrotor operates.

Figure 1 shows a sketch of the quadrotor setup, together with the force generated by each motor F_i and the direction of rotation for each propeller. The bijective correspondence between the motor forces and the total thrust T and torque

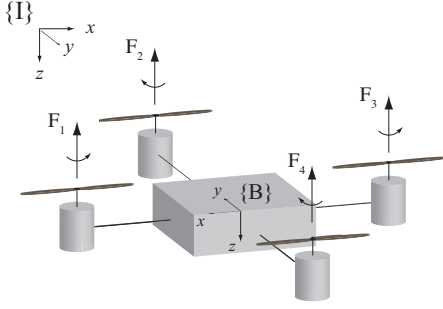


Fig. 1. Quadrotor vehicle setup.

$\mathbf{n} = [n_1 \ n_2 \ n_3]^T$ is given by (5)-(8), where k_{n_i} are constants intrinsic to the vehicle.

$$T = F_1 + F_2 + F_3 + F_4, \quad (5)$$

$$n_1 = k_{n_1}(F_4 - F_2), \quad (6)$$

$$n_2 = k_{n_2}(F_1 - F_3), \quad (7)$$

$$n_3 = k_{n_3}(F_1 + F_3 - F_2 - F_4). \quad (8)$$

The external force in body coordinates is given by

$$\mathbf{f} = -T\mathbf{u}_3 + mgR^T\mathbf{u}_3 \quad (9)$$

where $\mathbf{u}_3 = [0 \ 0 \ 1]^T$ and g is the gravitational acceleration. The quadrotor is thus an underactuated vehicle, as evidenced by (4) and (9), making the control problem much more difficult to address than what it would be for a fully-actuated vehicle. In this particular case we only have one degree of freedom for the force actuation in body frame and we are required to control the linear position of the vehicle $\mathbf{p} \in \mathbb{R}^3$.

III. PAN AND TILT CAMERA

Consider the quadrotor equipped with a pan and tilt camera and flying over a flat terrain with landmarks. Let $\{I\}$ be the inertial frame and $\{C\}$ the camera frame with origin at the camera's center of projection with the z -axis aligned with the optical axis. The observed scene consists of four points, which we call landmarks, whose 3-D coordinates in $\{I\}$ are denoted by ${}^I\mathbf{x}_i \in \mathbb{R}^3$, $i \in \{1, \dots, 4\}$. The 2-D image coordinates of these points are denoted by $\mathbf{y}_i \in \mathbb{R}^2$, $i \in \{1, \dots, 4\}$. Without loss of generality, the origin of $\{I\}$ is assumed to coincide with the centroid of the landmarks so that $\sum_{i=1}^4 {}^I\mathbf{x}_i = 0$ and the landmarks are assumed to belong to the x - y plane.

The image-based control problem considered consists in driving the image of the centroid of the landmarks, denoted by $\bar{\mathbf{y}}$, to the origin of the image plane by controlling the camera's pan and tilt angles. In general, the image of the landmarks' centroid does not coincide with the centroid of the images. For that reason, before proceeding, we highlight the fact that the image of the features' centroid $\bar{\mathbf{y}}$ can nonetheless be easily obtained from the images of each landmark \mathbf{y}_i . Noting that the feature centroid lies at the intersection between the vectors $\mathbf{x}_3 - \mathbf{x}_1$ and $\mathbf{x}_4 - \mathbf{x}_2$ and the intersection between lines is clearly an image invariant, we can immediately conclude that the image of the centroid $\bar{\mathbf{y}}$ coincides with the point at the intersection between the line segments $\mathbf{y}_3 - \mathbf{y}_1$ and $\mathbf{y}_4 - \mathbf{y}_2$ (see Fig. 2).

The camera can describe pan and tilt motions corresponding to the angles α and β , respectively. The origins of both

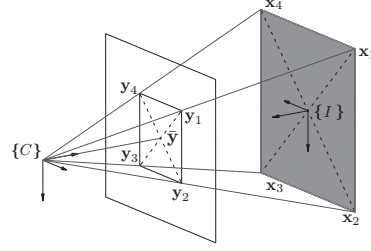


Fig. 2. Projection of the visual features in the image plane.

$\{B\}$ and $\{C\}$ are coincident and the rotation matrix from $\{C\}$ to $\{B\}$ is given by

$${}^B\mathbf{R} = R_{\text{pan}}R_{\text{tilt}}, \quad (10)$$

$$R_{\text{pan}} = \mathbf{R}_x(\alpha), \quad R_{\text{tilt}} = \mathbf{R}_y(\beta)$$

where $\mathbf{R}_x(\cdot)$ and $\mathbf{R}_y(\cdot)$ denote rotation matrices about the x -axis and y -axis, respectively.

We denote the configuration of $\{C\}$ with respect to $\{I\}$ by $({}^I_C R, {}^I\mathbf{p}_C) \in \text{SE}(3)$, where ${}^I_C R$ is the rotation matrix from $\{C\}$ to $\{I\}$ and ${}^I\mathbf{p}_C$ the position of the origin of $\{C\}$ with respect to $\{I\}$. Then, the 3-D coordinates of the feature points expressed in $\{C\}$ can be written as $\mathbf{r}_i = {}^I_C R^T {}^I\mathbf{x}_i + {}^I\mathbf{p}_C$, $i \in \{1, \dots, 4\}$ and, using the perspective camera model [16], the 2-D image coordinates of those points $\mathbf{y}_i \in \mathbb{R}^2$ can be written as

$$\begin{bmatrix} \mathbf{y}_i \\ 1 \end{bmatrix} = \delta_i \mathbf{A} \mathbf{r}_i,$$

where $\mathbf{A} \in \mathbb{R}^{3 \times 3}$ is the camera calibration matrix assumed to be known and δ_i is an unknown scalar encoding depth information and given by $\delta_i = (\mathbf{u}_3^T \mathbf{r}_i)^{-1}$, $\mathbf{u}_3 = [0 \ 0 \ 1]^T$.

The camera frame attitude kinematics can be described by

$${}^I_C \dot{\mathbf{R}} = {}^I_C \mathbf{R} S(\boldsymbol{\omega}_C),$$

where $\boldsymbol{\omega}_C \in \mathbb{R}^3$ denotes the camera angular velocity. Taking the time derivative of (10), and noting that ${}^I_C \mathbf{R} = {}^I_B \mathbf{R}_C^B \mathbf{R}$, straightforward computations show that $\boldsymbol{\omega}_C$ can be written as

$$\boldsymbol{\omega}_C = {}^C_B \mathbf{R} \boldsymbol{\omega}_B + R_{\text{tilt}}^T [\dot{\alpha} \ \dot{\beta} \ 0]^T, \quad (11)$$

where $\dot{\alpha}$ and $\dot{\beta}$ are the time derivatives of the camera pan and tilt angles, respectively.

In summary, to develop an active vision system using the camera pan and tilt degrees of freedom, we consider the following problem.

Problem 1: Let $\bar{\mathbf{y}}$ be the image of the landmarks' centroid given by $[\bar{\mathbf{y}}^T \ 1]^T = \delta \mathbf{A} \bar{\mathbf{r}}$, where $\bar{\mathbf{r}} = -{}^I_C R^T {}^I\mathbf{p}_C$ denotes the position of $\{I\}$ expressed in $\{C\}$ and $\delta = (\mathbf{u}_3^T \bar{\mathbf{r}})^{-1}$. Design a control law for $\dot{\alpha}$ and $\dot{\beta}$ based on the measurements of $\boldsymbol{\omega}_B$ and \mathbf{y}_i , $i \in \{1, \dots, 4\}$, such that $\bar{\mathbf{y}}$ approaches the center of the image plane.

A. Camera Pan and Tilt Controller

We resort to Lyapunov theory and consider the following candidate Lyapunov function

$$W = \frac{1}{2} \bar{\mathbf{r}}^T \Pi \bar{\mathbf{r}} = \frac{1}{2} (r_x^2 + r_y^2), \quad (12)$$

where $\bar{\mathbf{r}} = [r_x \ r_y \ r_z]^T$ and $\Pi \in \mathbb{R}^{3 \times 3}$ is the x - y plane projection matrix. Using the expression for $\boldsymbol{\omega}_C$ given in (11), the camera position kinematics can be written as

$$\begin{aligned} \dot{\bar{\mathbf{r}}} &= S(\bar{\mathbf{r}})\boldsymbol{\omega}_C - \mathbf{v} \\ &= S(\bar{\mathbf{r}})(R_{\text{tilt}}^T R_{\text{pan}}^T \boldsymbol{\omega}_B + R_{\text{tilt}}^T [\dot{\alpha} \ \dot{\beta} \ 0]^T) - \mathbf{v}, \end{aligned} \quad (13)$$

where \mathbf{v} is the camera linear velocity. Recall that by definition $\bar{\mathbf{r}}$ coincides with the position of the features' centroid and its image is given by $\bar{\mathbf{r}}$. Therefore, by guaranteeing that the Lyapunov function W is decreasing, or equivalently $[r_x \ r_y]$ is approaching the origin, we can ensure that $\bar{\mathbf{y}}$ is approaching the center of the image plane. To simplify the notation and without loss of generality, assume from now on that $\mathbf{A} = \mathbf{I}$ so that $\bar{\mathbf{y}} = [r_x \ r_y]^T / r_z$.

Lemma 2: Let the camera position kinematics be described by (13) and assume that the rigid body and camera motions are such that $r_z > 0$ and $\cos \beta \neq 0$. Consider the control law for the camera pan and tilt angular velocities given by

$$\begin{bmatrix} \dot{\alpha} \\ \dot{\beta} \end{bmatrix} = k_c \begin{bmatrix} 0 & -\frac{1}{\cos \beta} \\ 1 & 0 \end{bmatrix} \bar{\mathbf{y}} - \begin{bmatrix} 1 & 0 & -\tan \beta \\ 0 & 1 & 0 \end{bmatrix} R_{\text{pan}}^T \boldsymbol{\omega}_B, \quad (14)$$

where $k_c > 0$. Then, the time derivative of the Lyapunov function W along the system trajectories satisfies

$$\dot{W} \leq -(k_c - \epsilon)W, \quad \forall \|\Pi \bar{\mathbf{r}}\| \geq \frac{1}{\epsilon} \|\Pi \mathbf{v}\|, \quad (15)$$

and $0 < \epsilon < k_c$.

Proof: Taking the time derivative of (12) and using the expressions for $\dot{\bar{\mathbf{r}}}$ given in (13), we obtain

$$\begin{aligned} \dot{W} &= \bar{\mathbf{r}}^T \Pi (r_z S(\mathbf{u}_3) \boldsymbol{\omega}_C - \mathbf{v}) \\ &= r_z [r_y \ -r_x \ 0] R_{\text{tilt}}^T (R_{\text{pan}}^T \boldsymbol{\omega}_B + [\dot{\alpha} \ \dot{\beta} \ 0]^T) - \bar{\mathbf{r}}^T \Pi \mathbf{v}. \end{aligned}$$

Choosing $\dot{\alpha}$ and $\dot{\beta}$ such that

$$R_{\text{tilt}}^T (R_{\text{pan}}^T \boldsymbol{\omega}_B + [\dot{\alpha} \ \dot{\beta} \ 0]^T) = -k_c [\bar{y}_y \ -\bar{y}_x \ \kappa]^T, \quad (16)$$

for some κ yields $\dot{W} = -k_c W - \bar{\mathbf{r}}^T \Pi \mathbf{v}$ and consequently (15) holds. Solving (16) for $\dot{\alpha}$, $\dot{\beta}$, and κ , we obtain the control law (14). ■

Remark 3: If we apply the control law (14) to the system with state $\Pi \bar{\mathbf{r}} = [r_x \ r_y]^T$ and interpret \mathbf{v} as input, it follows from (15) that the system is exponentially input-to-state stable (ISS). As such, the distance between the image of the centroid $\bar{\mathbf{y}}$ and the origin is ultimately bounded by $\|\Pi \mathbf{v} / r_z\|$ and converges exponentially fast to that bound. Moreover, if $\Pi \mathbf{v} / r_z$ converges to zero so does $\bar{\mathbf{y}}$.

IV. QUADROTOR CONTROLLER

The control objective consists of designing a control law for the quadrotor actuations \mathbf{f} and \mathbf{n} , which ensures the convergence of the horizontal position in frame $\{I\}$ to zero with the largest possible basin of attraction, while maintaining the landmarks visible in the image sensor and the vehicle's vertical coordinate stable.

As sensor measurements we consider the image coordinates of the landmarks to be available for feedback in addition to the vehicle's attitude and angular velocity. Moreover, we consider the vehicle equipped with an absolute vertical position sensor. The vertical position sensor here considered can be a simple barometric sensor, providing the vehicle altitude, which differs from the distance to the ground.

To achieve the stabilization goal, the proposed controller also uses for feedback partial information on the position and body linear velocity, which are not directly available from the sensor measurements. The 2-D image coordinates of the landmarks' \mathbf{y}_i together with the rotation matrices ${}^B R$ and ${}^C R$ provide us with means of obtaining, up to a scale factor, the position \mathbf{p} and the body linear velocity ${}^I \mathbf{v} = [{}^I v_x \ {}^I v_y \ {}^I v_z]$, both expressed in the inertial frame. For that purpose, we first determine the direction of the landmarks, or more precisely their position up to a scale factor with respect to the body, expressed in the inertial frame. To simplify the necessary notation we introduce a new reference frame $\{L\}$, with the same origin as $\{B\}$ but with the orientation of $\{I\}$. Let $[x_i \ y_i \ z]^T = {}^I C R \mathbf{q}_i$ be the coordinates of the landmarks expressed in $\{L\}$. Choosing $1/z$ as the scale factor, the direction of the landmarks in frame $\{L\}$ can be obtained from

$$\begin{bmatrix} x_i/z \\ y_i/z \\ 1 \end{bmatrix} = \frac{{}^L C R [y_i^T \ 1]^T}{{}^L C R [y_i^T \ 1]^T} \triangleq \mathbf{s}_i. \quad (17)$$

The \mathbf{s}_i points can be thought as the images of the landmarks in a *virtual* camera, attached to the vehicle but with a fixed attitude relative to the inertial frame. Moreover, the position of the vehicle can be estimated up to a scaling factor by computing (17) with $\bar{\mathbf{y}}$. Taking the time derivative of (17), the following relation is obtained for the vehicle velocities, expressed either in $\{L\}$ or $\{I\}$,

$$\begin{bmatrix} \frac{{}^I v_x}{z} - \frac{x_i {}^I v_z}{z^2} \\ \frac{{}^I v_y}{z} - \frac{y_i {}^I v_z}{z^2} \\ 0 \end{bmatrix} = \dot{\mathbf{s}}_i, \quad (18)$$

where the right-hand-side derivative is a function of the measured variables ${}^L C R = {}^I C R$, $\boldsymbol{\omega}_C$, \mathbf{y}_i , and $\dot{\mathbf{y}}_i$.

Since (18) is valid for every landmark, the vehicle velocity can be partially recovered from the $\dot{\mathbf{s}}$ measurements by solving an overdetermined equation system in order to obtain a least squares solution for ${}^I \mathbf{v} / z$. This solution is akin to the computation performed in [7] to obtain ${}^I \mathbf{v} / z$ based on the derivative of the average of spherical images of features.

The methodology adopted to address the quadrotor vehicle control is in line with the state feedback controller proposed in [14]. However, as the full system state is not directly available for feedback, the controller is modified to use the image measurements and attitude information to stabilize the quadrotor position at the desired location.

The proposed controller makes use of the *unit quaternions* to represent the attitude, in contrast with the rotation matrix parametrization used previously. As attitude representation, the unit quaternion $\mathbf{q} \in \mathbb{S}^4$ is written in the form $\mathbf{q} = [q_0 \ q^T]^T$. The *scalar* part $q_0 \in \mathbb{R}$ is related to the rotation angle $\theta \in [0, \pi)$ and the *vector* part $q = [q_1 \ q_2 \ q_3]^T \in \mathbb{R}^3$ to the axis of rotation $\mathbf{n} \in \mathbb{S}^3$. The two representations relate through

$$\mathbf{q}(\theta, \mathbf{n}) = \begin{bmatrix} q_0 \\ q \end{bmatrix} = \begin{bmatrix} \cos(\theta/2) \\ \mathbf{n} \sin(\theta/2) \end{bmatrix}.$$

The controller comprises a vertical stabilization law together with a lateral-longitudinal-attitude stabilization law.

This latter law enforces two-time scale dynamics and decouples the lateral-longitudinal dynamics from the attitude dynamics.

A. Stabilization of the Vertical Error Dynamics

The vertical position sensor provides the altitude of the vehicle with respect to a standard reference (e.g. the GPS WGS84 ellipsoidal altitude). Hence, the control objective is to drive the vehicle to a give reference altitude h^* . Let h_0 be the altitude of frame $\{I\}$. Then, the altitude of the vehicle and its height in the inertial frame are related by

$$h(t) = h_0 - z(t),$$

where $z(t)$ is the z -coordinate of the vehicle in frame $\{I\}$. The dynamic equation for the altitude,

$$m\ddot{h} = (1 - 2q_1^2 - 2q_2^2)T - mg, \quad (19)$$

is derived from the altitude definition and the linear dynamics of the vehicle system represented in (2) and (4). The control law for the thrust T drives the vehicle to a fixed altitude h^* through

$$T = \frac{mg - k_1 e_1 - k_2 e_2}{1 - \text{sat}_c(2q_1^2 + 2q_2^2)} \quad (20)$$

where $e_1 = h - h^*$ and $e_2 = -\dot{e}_1/z$ are vertical errors, k_1 and k_2 are positive parameters, and $\text{sat}_c(x)$ with $0 < c < 1$ is a saturation function defined as

$$\text{sat}_c(x) = \begin{cases} x, & \text{if } |x| \leq c \\ c \text{sign}(x), & \text{otherwise} \end{cases}$$

The saturation function ensures that the thrust control law (20) is well posed for any attitude of the vehicle. The subsequent choice of the attitude control law guarantees that there exists a time $T^* > 0$ such that for all $t > T^*$, $2q_1(t)^2 + 2q_2(t)^2 < c$. For $t > T^*$, the altitude dynamics simplify to the error dynamics

$$m\ddot{e}_1 = -k_1 e_1 - \frac{k_2}{e_1 + h^* - h_0} \dot{e}_1, \quad (21)$$

which amount to a double integrator driven by a PD controller with variable derivative gain. It is well known that if the controller is well defined for all time, meaning that $e_1(t) + h^* - h_0 < 0$ or equivalently $h(t) > h_0$ and $z(t) < 0$ for all time, then the error system (19) has an exponentially stable equilibrium point at the origin [17]. In the following Lemma, we define simple initial conditions under which the controller is well defined.

Lemma 4: Consider the dynamic system described by (21) with $e_1(t) = h(t) - h^* = h_0 - z(t) - h^*$ and $k_1, k_2 > 0$. If the initial conditions verify $z(0) < 0$ then $z(t) < 0$ for all time.

Proof: Consider the dynamic system rewritten as

$$m(e_1 + h^* - h_0)\ddot{e}_1 + k_1(e_1 + h^* - h_0)\dot{e}_1 + k_2\dot{e}_1 = 0.$$

Integrating both sides we obtain

$$k_2(e_1 + h^* - h_0)e^{\frac{1}{k_2}(\dot{e}_1 + k_1 \int e_1)} = C$$

where $C \in \mathbb{R}$ is an integration constant. Noticing that $z(t) = -(e_1(t) + h^* - h_0)$ then $z(0) < 0$ results in $z(t) < 0$ for all time $t > 0$. ■

A corollary of this Lemma is that using the thrust control law (20) a collision with the ground (crossing of $z = 0$) is guaranteed not to occur for $2q_1(t)^2 + 2q_2(t)^2 < c$.

B. Stabilization of the Lateral and Longitudinal Dynamics

To stabilize the quadrotor in hover, the vertical stabilizer (20) needs to be combined with a controller for the torque actuation \mathbf{n} that stabilizes both the attitude and the lateral-longitudinal dynamics. The proposed control law simultaneously achieves the condition $2q_1(t)^2 + 2q_2(t)^2 < c$ in finite time, stabilizes the lateral and longitudinal dynamics, and ensures $q_0(t) > \epsilon$ for all time. To achieve these goals we interpret the attitude as a *virtual control* for the lateral-longitudinal dynamics. In this setting the attitude follows the virtual control law with fast dynamics and a slower outer control loop generates the virtual control for the attitude so as to stabilize the lateral-longitudinal dynamics.

The lateral-longitudinal-attitude dynamics of the quadrotor vehicle, with the thrust defined as (20), are described by the following system of equations

$$\dot{y} = v_y \quad (22)$$

$$m\dot{v}_y = d(\mathbf{q})q_1 + m(\mathbf{q})q_2q_3 + \delta_y \quad (23)$$

$$\dot{x} = v_x \quad (24)$$

$$m\dot{v}_x = -d(\mathbf{q})q_2 + m(\mathbf{q})q_1q_3 + \delta_x \quad (25)$$

$$\dot{q}_0 = -\frac{1}{2}q^T \boldsymbol{\omega}_B \quad (26)$$

$$\dot{q} = \frac{1}{2}(q_0 \mathbf{I} + S(q))\boldsymbol{\omega}_B \quad (27)$$

$$\mathbb{J}\dot{\boldsymbol{\omega}}_B = -S(\boldsymbol{\omega}_B)\mathbb{J}\boldsymbol{\omega}_B + \mathbf{n} \quad (28)$$

where components x, y, v_x and v_y are written in frame $\{I\}$,

$$d(\mathbf{q}) = \frac{2mgq_0}{1 - \text{sat}_c(2q_1^2 + 2q_2^2)}, \quad (29)$$

$$m(\mathbf{q}) = -\frac{2mg}{1 - \text{sat}_c(2q_1^2 + 2q_2^2)},$$

and δ_x, δ_y are asymptotically vanishing signals defined as

$$\delta_x = \frac{2q_1q_3 + 2q_0q_2}{1 - \text{sat}_c(2q_1^2 + 2q_2^2)}(-k_1 e_1 - k_2 e_2),$$

$$\delta_y = \frac{2q_2q_3 - 2q_0q_1}{1 - \text{sat}_c(2q_1^2 + 2q_2^2)}(-k_1 e_1 - k_2 e_2).$$

The control law for the attitude subsystem is chosen as the proportional-differential law

$$\mathbf{n} = K_P(\eta - K_D\boldsymbol{\omega}_B) \quad (30)$$

where $K_P > 0$ and $K_D > 0$ are design parameters and $\eta = q^* - q$ is the attitude error with q^* defined as the virtual control for the $x - y$ system.

According to Proposition 5.7.1 in [14], which we now restate for the sake of completeness, proper tuning of the torque control law (30) ensures boundedness of the attitude subsystem trajectories and consequent stabilization of the vertical error dynamics.

Proposition 5: For $0 < \epsilon < 1$, fix compact sets of initial conditions \mathcal{Q}, Ω for $q(t)$ and $\boldsymbol{\omega}_B(t)$, respectively, such that

$$\mathcal{Q} \subset \{q \in \mathbb{R}^3 : \|q\| < \sqrt{1 - \epsilon^2}\}.$$

Then, for any $T^* > 0$ there exist $K_D^* > 0$ and positive numbers $K_P^*(K_D^*), \lambda^*(K_D^*)$ such that, for any initial conditions $(q(0), \boldsymbol{\omega}_B(0)) \in \mathcal{Q} \times \Omega$ and $\|q^*(t)\| < \lambda^*$, the trajectories of the attitude subsystem (26)-(28) in closed-loop with controller (30) are bounded, satisfy $q_0(t) > \epsilon$ for all time, and verify $2q_1^2 + 2q_2^2 < c$, for all $t \geq T^*$.

To achieve convergence of the overall system, the virtual control q^* is generated from the quadrotor position and velocities by a *nested saturation* control law. Consider the new state variables

$$\zeta_1 = \frac{1}{z} \begin{bmatrix} y \\ x \end{bmatrix}, \quad \zeta_2 = \frac{1}{z} \begin{bmatrix} v_y \\ v_x \end{bmatrix} + \lambda_1 \sigma\left(\frac{K_1}{\lambda_1} \zeta_1\right) - \frac{v_z}{z} \zeta_1,$$

and fix for q^* the nested saturation structure

$$q^* = -P_2 \lambda_2 \sigma\left(\frac{K_2}{\lambda_2} \zeta_2\right), \quad (31)$$

where

$$P_2 = \begin{bmatrix} 1 & 0 \\ 0 & -1 \\ 0 & 0 \end{bmatrix}$$

and $\sigma(\mathbf{x}) = (\sigma(x_1), \dots, \sigma(x_n))$ is a sigmoidal saturation function (see [14]).

Notice that the states ζ_1 and ζ_2 , and consequently q^* , are readily obtained from the camera sensor through (17), using $\bar{\mathbf{y}}$ and the relation between positions ${}^L \mathbf{p}_B = -{}^L \mathbf{p}_I$, and through (18), using

$$\frac{1}{z} \begin{bmatrix} v_y \\ v_x \end{bmatrix} - \frac{v_z}{z} \zeta_1 = \begin{bmatrix} \frac{v_x}{z} - \frac{x v_z}{z^2} \\ \frac{v_y}{z} - \frac{y v_z}{z^2} \end{bmatrix}.$$

The time derivatives of the states are

$$\begin{aligned} \dot{\zeta}_1 &= \zeta_2 - \lambda_1 \sigma\left(\frac{K_1}{\lambda_1} \zeta_1\right), \\ m \dot{\zeta}_2 &= \frac{D}{z} \left(-P_2 \lambda_2 \sigma\left(\frac{K_2}{\lambda_2} \zeta_2\right) + \eta \right) \\ &\quad + m K_1 \sigma'\left(\frac{K_1}{\lambda_1} \zeta_1\right) \dot{\zeta}_1 + \delta + \delta_2, \end{aligned}$$

where

$$D = \begin{bmatrix} d(\mathbf{q}) & m(\mathbf{q})q_3 & 0 \\ m(\mathbf{q})q_3 & -d(\mathbf{q}) & 0 \end{bmatrix}$$

and the exogenous inputs δ and δ_2 are given by

$$\delta = \begin{bmatrix} \delta_x \\ \delta_y \end{bmatrix} / z, \quad \delta_2 = \frac{k_1 e_1 + k_2 e_2}{z} \zeta_1 + m \frac{v_z^2}{z^2} \zeta_1 - m \frac{v_z}{z} \dot{\zeta}_1.$$

From the exponential convergence to zero of e_1 , e_2 , v_z and noting that the growth of $\|\zeta_1\|$, $\|\zeta_2\|$ is at most quadratic, we can assert that the exogenous inputs are asymptotically vanishing and converge exponentially fast to zero for $t > T^*$.

From definition (29) and the vertical controller we have

$$0 < d^L \leq d(\mathbf{q}, t) \leq d^U, \quad 0 < z^L < z(t) < z^U.$$

where $z(t)$ is the height of the vehicle with respect to the landmarks' centroid. The following result is an adaptation of Proposition 5.7.2 and Theorem 5.7.5 in [14] and gives guarantees for the proposed quadrotor stabilization law.

Theorem 6: Let K_D be fixed according to Proposition 5 and let K_i^* and λ_i^* , $i = 1, 2$, be such that the following inequalities are satisfied

$$\frac{\lambda_2^*}{K_2^*} < \frac{\lambda_1^*}{4}, \quad 4\lambda_1^* K_1^* < \frac{1}{m} \frac{d^L}{z^U} \frac{\lambda_2^*}{8}, \quad 24 \frac{K_1^*}{K_2^*} < \frac{1}{6} \frac{d^L}{d^U} \frac{z^L}{z^U}. \quad (32)$$

Then, there exist positive numbers K_P^* and ϵ^* such that, taking

$$\lambda_i = \epsilon^i \lambda_i^* \text{ and } K_i = \epsilon K_i^*, \quad i = \{1, 2\}, \quad (33)$$

for all $K_P > K_P^*$ and $0 < \epsilon \leq \epsilon^*$, the state trajectories of the system (22)-(28) in closed-loop with the controller defined by

(20), (30) and (31) converge asymptotically to the origin¹ for any initial condition $z(0) \in \mathcal{Z}$, $(x(t), v_x(t), y(t), v_y(t)) \in \mathbb{R}^4$ and $(q(0), \omega_B(0)) \in \mathcal{Q} \times \Omega$ with $q_0 > 0$.

Proof: The proof follows from the arguments in [14] where the statement is proven for constant $z(t) = Z$ and exogenous disturbance $\delta_2(t) = 0$. The statement of Theorem 6 is proven by noting that the additional disturbance $\delta_2(t)$ is asymptotically vanishing. The lateral-longitudinal subsystem does not have finite escape time and the trajectory $(\zeta_1(t), \zeta_2(t))$ exists and is bounded for $t > 0$. Since the disturbance $\delta_2(t)$ is asymptotically vanishing, there exists a finite time $T > 0$ such that the disturbances are within the bounds for which the convergence of (ζ_1, ζ_2) to zero is ensured by using gains (33), verifying (32). The remainder of the claims in the theorem statement follows identically from [14]. ■

Gathering the previous results, we can now state the following theorem which summarizes the main results of the paper and corresponds to the control architecture represented in Fig. 3.

Theorem 7: Consider a quadrotor described by the dynamic system (1)-(4) equipped with a pan and tilt camera modeled by (10) and (11) and apply the set of controllers (14), (20), (30) and (31). Then, for any initial condition $z(0) \in \mathcal{Z}$, $(x(t), v_x(t), y(t), v_y(t)) \in \mathbb{R}^4$, $(q(0), \omega_B(0)) \in \mathcal{Q} \times \Omega$ with $q_0 > 0$ such that the landmarks are visible in the image sensor, the vehicle's position, attitude, velocities converge asymptotically to ${}^L \mathbf{p}_B = [0 \ 0 \ h^* - h_0]^T$, ${}^L R = I_3$, $\mathbf{v}_B = 0$, $\omega_B = 0$, respectively, whereas the camera's velocity and image coordinates converge to $\omega_C = 0$ and $\bar{\mathbf{y}} = 0$, respectively.

Proof: The stated result follows immediately from Theorem 6 and Lemma 2. Theorem 6 states that convergence of the vehicle position and velocity to zero is achieved and, through Lemma 2, convergence of the landmarks' centroid image coordinates to zero is achieved if the vehicle velocity converges to zero. ■

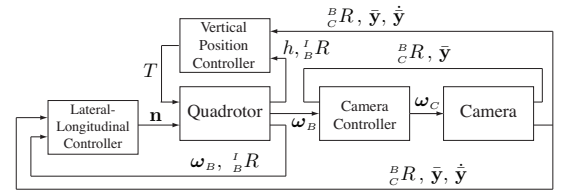


Fig. 3. Block diagram of the control architecture.

V. SIMULATION RESULTS

In this section we present the results from a simulation run of the proposed control architecture. At the initial configuration the quadrotor is at rest. The camera points towards a set of landmarks that are visible and the centroid of the landmarks is not coincident with origin of the image plane. The objective of the simulation is to hover the quadrotor over the centroid of the landmarks at a reference vertical

¹That is, $(x(t), v_x(t), y(t), v_y(t), e_z(t), v_z(t), \mathbf{q}(t), \omega_B(t))$ converge asymptotically to $(0, 0, 0, 0, 0, 0, \mathbf{q}_i, \mathbf{0})$, where $\mathbf{q}_i = [1 \ 0 \ 0 \ 0]^T$.

position. The initial position of the quadrotor, expressed in $\{I\}$, is $\mathbf{p} = [10 \ -20 \ -5]^T$ m. The vehicle parameters are $m = 1$ kg, $\mathbb{J} = 0.5$ kg m², $\lambda_1 = 10$, $\lambda_2 = 0.3$, $K_1 = 0.3$, $K_2 = 0.3$, $K_P = 10$, $K_D = .5$, $k_1 = 0.1$, $k_2 = 6$ and $c = \cos(\pi/12)$.

Figure 4 presents the time evolution of the quadrotor position error expressed in inertial coordinates. We can verify that the error converges from the initial $\mathbf{e} = [10 \ -20 \ 5]^T$ m to zero and is negligible after about 20 seconds.

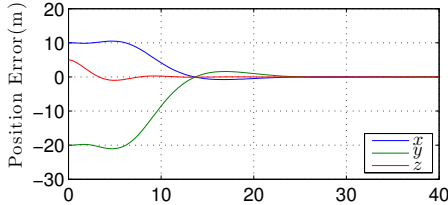


Fig. 4. Inertial position error of the quadrotor.

The quadrotor actuations are shown in Figure 5. The thrust initially overcomes gravity forcing the quadrotor to go up, and then, when the altitude stabilizes, the thrust also stabilizes to a steady-state value where it compensates the gravity. The high initial actuation for the torque drives the thrust vector to point in the direction of the landmarks. Once this is accomplished the torque actuations necessary to stabilize the vehicle are small, as can be observed in Figure 5.

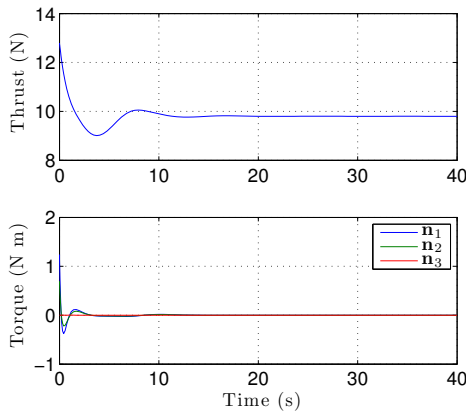


Fig. 5. Thrust and torque quadrotor actuations.

The position of the landmarks' centroid in the image plane is displayed in Figure 6. The centroid $\bar{\mathbf{y}}$ converges asymptotically to the origin as the velocity of the quadrotor converges asymptotically to zero. The disturbance effect of the quadrotor linear velocity on the time evolution of $\bar{\mathbf{y}}$ can be observed in the figure by noting that the convergence to the origin is not monotonic.

VI. CONCLUSIONS

This paper proposed a nonlinear control architecture for the stabilization of a quadrotor vehicle based on image measurements of a set of landmarks obtained from a pan and tilt camera. The vehicle was stabilized vertically to a given altitude with a PD control law based on image measurements

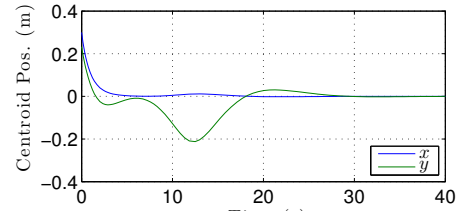


Fig. 6. Landmarks' centroid position in image coordinates.

and a vertical position sensor. The lateral-longitudinal stabilization was achieved with a nested saturation control law using feedback of the image measurements, body attitude and angular rate. During the whole stabilization procedure the pan and tilt camera was actuated so as to keep the image of the landmarks' centroid at the center of the image plane. Simulation results exhibited good performance and attested the applicability of the proposed technique.

REFERENCES

- [1] F. Chaumette and S. Hutchinson, "Visual servo control, part i: Basic approaches," *IEEE Robotics and Automation Magazine*, vol. 13, no. 4, pp. 82–90, December 2006.
- [2] —, "Visual servo control, part ii: Advanced approaches," *IEEE Robotics and Automation Magazine*, vol. 14, no. 1, pp. 109–118, March 2007.
- [3] N. Cowan, J. Weingarten, and D. Koditschek, "Visual servoing via navigation functions," *Robotics and Automation, IEEE Transactions on*, vol. 18, no. 4, pp. 521–533, Aug 2002.
- [4] R. Cunha, C. Silvestre, J. Hespanha, and A. Aguiar, "Vision-based control for rigid body stabilization," in *Decision and Control, 2007 46th IEEE Conference on*, Dec. 2007, pp. 2345–2350.
- [5] E. Malis and F. Chaumette, "Theoretical improvements in the stability analysis of a new class of model-free visual servoing methods," *Robotics and Automation, IEEE Transactions on*, vol. 18, no. 2, pp. 176–186, Apr 2002.
- [6] A. Aguiar and J. Hespanha, "Minimum-energy state estimation for systems with perspective outputs," *Automatic Control, IEEE Transactions on*, vol. 51, no. 2, pp. 226–241, Feb. 2006.
- [7] R. Mahony, P. Corke, and T. Hamel, "Dynamic image-based visual servo control using centroid and optic flow features," *Journal of Dynamic Systems, Measurement, and Control*, vol. 130, no. 1, p. 011005, 2008. [Online]. Available: <http://link.aip.org/link/?JDS/130/011005/1>
- [8] R. Mahony and T. Hamel, "Image-based visual servo control of aerial robotic systems using linear image features," *Robotics, IEEE Transactions on*, vol. 21, no. 2, pp. 227–239, April 2005.
- [9] Y. Ma, J. Kosecka, and S. Sastry, "Vision guided navigation for a nonholonomic mobile robot," *Robotics and Automation, IEEE Transactions on*, vol. 15, no. 3, pp. 521–536, Jun 1999.
- [10] O. Tahri and F. Chaumette, "Point-based and region-based image moments for visual servoing of planar objects," *Robotics, IEEE Transactions on*, vol. 21, no. 6, pp. 1116–1127, Dec. 2005.
- [11] R. Vidal, O. Shakernia, and S. Sastry, "Following the flock [formation control]," *Robotics & Automation Magazine, IEEE*, vol. 11, no. 4, pp. 14–20, Dec. 2004.
- [12] E. Frazzoli, M. Dahleh, and E. Feron, "Trajectory tracking control design for autonomous helicopters using a backstepping algorithm," in *American Control Conference, 2000. Proceedings of the 2000*, vol. 6, 2000, pp. 4102–4107 vol.6.
- [13] D. Cabecinhas, R. Cunha, and C. Silvestre, "Trajectory tracking control for quadrotors," *European Control Conference*, 2009.
- [14] A. Isidori, L. Marconi, and A. Serrani, *Robust Autonomous Guidance*. Springer, 2003.
- [15] L. Marconi and R. Naldi, "Robust full degree-of-freedom tracking control of a helicopter," *Automatica*, vol. 43, no. 11, pp. 1909 – 1920, 2007.
- [16] H. Rehlinger and B. K. Ghosh, "Pose estimation using line-based dynamic vision and inertial sensors," *IEEE Transactions on Automatic Control*, vol. 48, no. 2, pp. 186–199, 2003.
- [17] H. K. Khalil, *Nonlinear systems; 3rd ed.* Upper Saddle River, NJ: Prentice-Hall, 2002, order from outside CERN via Inter Library Loan.